Exonuclease−Polymerase Active Site Partitioning of Primer−Template DNA Strands and Equilibrium Mg^{2+} Binding Properties of Bacteriophage T4 DNA Polymerase†

Joseph M. Beechem,*,‡ Michael R. Otto,‡,§ Linda B. Bloom,||,⊥ Ramon Eritja,@ Linda J. Reha-Krantz,# and Myron F. Goodman||

Department of Molecular Physiology and Biophysics, Vanderbilt University, Nashville, Tennessee 37232, Department of Biological Sciences, University of Alberta, Edmonton, Alberta, Canada T6G 2E9, European Molecular Biology Organization, Heidelburg, Germany, and Department of Biological Sciences, HEDCO Molecular Biology Laboratory, University of Southern California, Los Angeles, California 90089-1340

Received January 9, 1998; Revised Manuscript Received May 15, 1998

ABSTRACT: The binding of bacteriophage T4 DNA polymerase (T4 pol) to primer−template DNA with 2-aminopurine (2AP) located at the primer terminus results in the formation of a hyperfluorescent 2AP state. Changes in this hyperfluorescent state were utilized to investigate the fractional concentration of primer−templates bound at the exonuclease and statically quenched polymerase sites. In the absence of Mg^{2+}, a hydrophobic exonuclease site dominates over the polymerase site for possession of the primer terminus. The fractional concentration of primer termini in the exonuclease site was found to be 64 and 84% for correct (AP-T) and mismatched (AP-C) primer−templates, respectively. Exonuclease-deficient mutants, polymerase-switching mutants, and nucleoside triphosphates all shift this equilibrium toward the polymerase site. Synthesis of stereospecific hydrolysis resistant phosphorothioate 2AP-labeled DNA allowed Mg^{2+} ion binding titrations to be performed in the presence of bound DNA without the complication of the excision reaction. High- and low-affinity Mg^{2+} binding sites were observed in the presence of bound double-stranded (ds) DNA, with dissociation constants in the micromolar (WT $K_d = 5.1\ \mu M$) and millimolar (WT $K_d = 2.5$ mM) concentration ranges. Mg^{2+} binding was found to be a key "conformational switch" for T4 pol. As the high-affinity Mg^{2+} binding sites are filled, the primer terminus migrates from the exonuclease site to a highly based stacked polymerase active site. Filling the low-affinity Mg^{2+} sites further shifts the primer terminus into the polymerase site. As the low-affinity Mg^{2+} sites are filled, T4 pol "loosens its grip" on the primer terminus, as shown by a large amplitude increase in the nanosecond rotational mobility of 2AP within the bound T4 complex. The hyperfluorescent exonuclease site is spatially localized to 2AP positioned on the primer end. The penultimate ($n - 1$) position, as well as $n - 2$ and $n - 5$ positions, reveals no detectable fluorescent enhancement upon binding. The observed position-dependent fluorescence data, when combined with time-resolved total-intensity and anisotropy data, suggest that the creation of the hyperfluorescent state is caused by phenylalanine 120 (F120) of T4 pol intercalating into 2AP primers much like that observed for phenylalanine 123 of RB69 DNA polymerase intercalating into deoxythymidine primers [Wang, J., et al. (1997) *Cell 89*, 1087−1099]. As Mg^{2+} binds in the exonuclease site of T4 pol, the primer terminus appears to be "pulled backward" into the active site, decreasing the concentration of F120-intercalated primer termini, and bringing the exonuclease active site residues closer to the primer terminus scissile phosphate bond.

Bacteriophage T4 DNA polymerase (T4 pol)[1] is a single polypeptide of 898 amino acid residues (104 kDa) which contains both 5′ → 3′ polymerase and 3′ → 5′ exonuclease active sites. Throughout DNA replication, proofreading of the primer−template end occurs using structural transitions in the protein−DNA complex which moves the primer terminus between the polymerase and exonuclease active sites. In the Klenow fragment, the primer terminus must be separated from the template strand and moved approximately 25 Å during this proofreading step (*1*). A movement of approximately 30 Å has been predicted for the highly

† This work was supported by NIH Grants GM45990, RR5823 (J.M.B.), and GM21422 (M.F.G.) and a NSERC collaborative grant (L.J.R.-K.).

* Corresponding author.

‡ Vanderbilt University. Both of these authors contributed equally to this work.

§ Present address: Axiom Biotechnologies, San Diego, CA 92121.

|| University of Southern California.

⊥ Present address: Department of Chemistry, Arizona State University, Tempe, AZ 85287.

@ European Molecular Biology Organization.

University of Alberta.

[1] Abbreviations: 2AP, 2-aminopurine; dAPMP, 2-aminopurine 2′-deoxyribonucleoside 5′-monophosphate; DTT, dithiothreitol; T4 pol, wild-type T4 DNA polymerase; WT, wild type; p/t, 17mer−30mer primer−template; ds, double-stranded; ss, single-stranded; exo⁻, 3′ → 5′ exonuclease-deficient T4 mutant; KF, Klenow fragment of *Escherichia coli* DNA polymerase I.

S0006-2960(98)00074-9 CCC: $15.00
Published on Web 06/25/1998

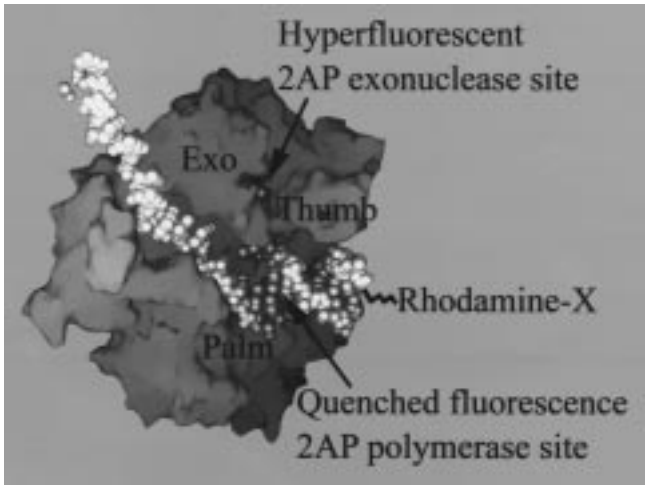

FIGURE 1: Site-specific location of the fluorescence probes utilized to study the equilibrium (this study) and kinetic aspects [following paper (*12*)] of processing single- and double-stranded DNA by T4 DNA polymerase (adapted from Figure 8 of ref *2*). The highly homologous RB69 DNA pol structure (*2*) is shown bound to p/t DNA. 2AP was site-specifically incorporated at the 3′-primer terminus and is hypothesized to partition between a hyperfluorescent state in the exonuclease binding site and a statically quenched polymerase site. The extrinsic fluorescent label rhodamine-X (Molecular Probes) was placed at the DNA 5′-end (via a six-carbon chain linker). Pre-steady-state kinetic studies (*12*) utilize both 2AP and rhodamine-X 5′-labeled DNA spectroscopic signals to simultaneously monitor both T4 pol binding and primer terminus base unstacking events.

homologous (to T4 pol) bacteriophage RB69 DNA polymerase (*2*). In this study, changes in 2AP fluorescence, site-specifically incorporated into the primer terminus and bound to T4 pol, are examined. The fluorescent quantum yield of 2AP is exquisitely sensitive to the vertical (i.e., same strand) DNA base-stacking environment (*3*), allowing a detailed examination of altered primer-strand base-stacking properties which occur during the 25−30 Å movements of the primer terminus back and forth between the polymerase and exonuclease sites (Figure 1).

The sequences of the exonuclease domains of DNA polymerases (in general) are very slightly homologous, yet the crystal structures of KF and T4 exonuclease domains are nearly identical (*4*, *5*). Although the structures of the 3′ → 5′ exonuclease active sites of KF and T4 pol are similar, hydrolysis rates are very different. T4 pol excises bases from DNA with rates 10^3 greater than that of the KF exonuclease (*6*−*11*).

In the crystal structure determination of the isolated exonuclease domain of T4 pol (*5*), important contact regions from the "missing" polymerase domain may have allowed the exonuclease domain to adopt a conformation different from the intact enzyme. In the structure of the T4-like RB69 DNA polymerase (*2*), the full polymerase and exonuclease domains of the DNA polymerase were present and revealed that the "tip" of the polymerase thumb domain forms the side wall of the single-stranded binding cleft of the exonuclease site (Figure 1). This thumb domain causes several key residues in the exonuclease domain to change position. Remarkably, phenylalanine 123 (F123) of RB69 DNA polymerase was found to intercalate into a bound ss primer (dT_{16}) in the exonuclease site between the 3′-primer terminus and the penultimate base. All of the data to be described in this and the following paper (*12*) are consistent with a similar intercalation event occurring in T4 pol, where it is proposed that F120 (of T4 pol) also intercalates into the primer terminus.

How the primer terminus migrates 25−30 Å between the exonuclease and polymerase sites has been the subject of extensive debate and investigation. This movement was originally thought to occur by the DNA sliding along its screw axis until the primer terminus was accessible to the exonuclease active site (*13*). Recent crystallographic results on DNA polymerase I (*14*) suggest that the duplex DNA appears to translate along the helix axis when the primer terminus moves from the pol to the exo sites. In RB69, it is hypothesized that the template strand is invariant, and only the primer strand "toggles" back and forth between the exonuclease and polymerase active sites (*2*). Given the complex nature of this active site switching event, it is anticipated that a large number of distinct protein conformational states will be required for each complete reaction cycle. By utilizing a fluorescence probe (2AP) which is both spectroscopically sensitive and an enzyme substrate, multiple intermediate states associated with DNA processing were quantitated. These experiments provide a unique site-specific approach for selectively monitoring the environment of a single DNA base as it is altered by a DNA polymerase.

Despite the intense interest in the role of Mg^{2+} in DNA polymerase reactions, no binding studies have ever been performed on a DNA polymerase when it has been saturated with ds or ss DNA (due to rapid hydrolysis of the DNA under these conditions). In this study, full equilibrium Mg^{2+} binding studies of T4 complexed with p/t DNA are reported. These binding studies were made possible by the synthesis of site-specific 2AP-containing DNA with stereospecific nonhydrolyzable phosphothioate linkages at both the 3′-primer and 3′-template ends.

The focus of this paper is an in-depth investigation of transitions between multiple p/t DNA polymerase−exonuclease states as a function of DNA p/t sequence, T4 polymerase mutants, and deoxynucleoside triphosphates, over a wide range of Mg^{2+} concentrations.

EXPERIMENTAL PROCEDURES

Materials

Preparation of WT and Mutant Polymerases. Wild-type T4 DNA polymerase and exonuclease-deficient mutants D112A/E114A, D324A, and D219A and the switching mutant L412M were prepared and purified as described previously (*15*, *16*). T4 polymerase and mutant concentrations were determined by the absorbance at 280 nm [1.5×10^5 M^{-1} cm^{-1} (*17*)]. Each preparation was titrated to determine the concentration of T4 pol necessary to completely bind p/t DNA as observed by the fluorescence change in 2AP at the primer end in the presence of EDTA (*11*).

Preparation of Oligonucleotides. Oligonucleotides were prepared using standard β-cyanoethyl phosphoramidite reagents from Applied Biosystems. 2AP was incorporated at the 3′-end of primers using a 2AP-derivatized CPG (*18*). Primer−template DNA with 2AP at interior positions was prepared using a custom synthesis 2AP−phosphoramidite. The majority of all studies were performed with the following

p/t DNA: primer (17mer), 5′-TCCCAGTCACGACGTC-2AP-3′; and template (30mer), 3′-AGGGTCAGTGCTG-CAG-T-AGTACGAGCTACT-5′.

Preparation of Hydrolysis Resistant Oligonucleotides. Hydrolysis resistant α-S-containing primer and template DNAs were prepared using a sulfurizing reagent (Glen Research, Sterling, VA) to protect both stands from the potent 3′ → 5′ exonuclease activity of T4 pol. Two diastereomers of the α-thio-DNA are generated during DNA synthesis. One diastereomer is rapidly hydrolyzed by the 3′ → 5′ exonuclease of T4 pol, while the other is extremely hydrolysis resistant. Following nonstereospecific synthesis, oligonucleotides were digested with T4 polymerase to remove the strands containing the hydrolyzable phosphorothioate linkage (∼50% of the synthesized oligonucleotide was digested during this step). The remaining diastereomer was extremely resistant to hydrolysis by T4 pol (≈3.0% hydrolyzed in a 24 h exposure). Several studies have shown that when the S_p nucleoside triphosphate isomer is incorporated into DNA using either Klenow Fragment or T4 polymerase (*19*, *20*), it can be excised by the 3′ → 5′ exonuclease activity of T4 pol. Since nucleotide incorporation occurs with inversion of configuration, the hydrolysis resistant isomer utilized in this study must contain a phosphorothioate linkage with an S_p configuration. Following digestion, the nucleotide monophosphates were removed using a P6 desalting gel (Bio-Rad, Richmond, CA), and the α-S (S_p configuration) oligos were further purified using polyacrylamide gel electrophoresis.

Methods

Steady-State Emission Spectra of WT and Mutant T4 Pol−DNA Complexes. Steady-state fluorescence emission spectra were collected from 330 to 460 nm on a SPEX 1681 Fluorolog spectrofluorometer. Sample excitation was at 317 nm. Solutions contained 0.5 μM DNA (ss primer or ds p/t), 2.0 μM WT or mutant T4 polymerase, 25 mM Hepes (pH 7.5), 50 mM NaCl, and 0.5 mM EDTA.

Positional Dependence of 2AP Fluorescence within DNA. The excitation wavelength was 310 nm, and the fluorescence emission was collected from 330 to 460 nm in 200 nM p/t, 800 nM T4 pol, 25 mM Hepes (pH 7.5), 50 mM NaCl, 0.5 mM EDTA, 0.5 mM DTT, and 5 mM KH_2PO_4. The background fluorescence from the T4 polymerase was subtracted from the fluorescence intensity of the T4 pol−DNA complex. The area under the emission spectra for each of the complexes was compared with that of the 2AP in the ds DNA alone to determine the fluorescence enhancement at the specific sites.

Determination of the Mg^{2+} Dissociation Constants for T4 Pol Bound to Nonhydrolyzable DNA. The fluorescence steady-state emission of T4 pol−DNA complexes was examined at an emission wavelength of 360 nm using 310 nm excitation. Solution conditions were 250 nm DNA, 1.5 μM T4 pol, 25 mM Hepes (pH 7.5), 50 mM NaCl, and 1 mM DTT. Experiments were performed with WT T4 pol and D219A, D324A, and D112A/E114A exo^- mutants. Solutions containing the divalent cation ($MgCl_2$) were titrated into the T4 pol−DNA complex (150 μL initial volume) in 3 μL aliquots. Absolute $MgCl_2$ concentrations were verified using a Molecular Probes Mg^{2+} calibration standard kit (product M-3120, Molecular Probes, Eugene, OR). The change in the fluorescence signal used to determine the dissociation constants was calculated by subtracting the background fluorescence of the polymerase in buffer alone, volume correcting the intensity, and dividing by the fluorescence signal for the T4 pol−DNA complex in the absence of Mg^{2+}. The fluorescence-intensity profiles were fit using a transform in Sigmaplot 4.1 (Jandel Scientific, San Rafael, CA) as a sum of one and/or two independent binding equilibria (*21*).

Time-Resolved Detection System and Measurements. The time-correlated single-photon counting detection setup is as described previously with the exceptions noted below (*22*). Excitation was provided by a Nd:YAG synchronously pumped dye laser (Coherent Lasers, Santa Clara, CA), frequency-doubled to produce 1 ps pulses (at 4 MHz) at 317.5 nm. Emission was collected through a 360 nm cuton filter and a SPEX 0.22 m monochromator set at 365 nm. The fluorescence total-intensity decay was calculated from the vertical and horizontal polarized emissions. Nonlinear data analysis was performed in terms of sums-of-exponentials models using the Globals Unlimited software (Urbana, IL) (*23*). Standard statistical tests (*24*) were utilized to determine the minimum number of exponential components required to adequately represent the data (examination of the χ^2 value, distribution of residuals, autocorrelation of residuals, runs test, etc.).

Lifetime measurements of hydrolyzable DNA (in the absence of T4 pol) were performed in 25 mM Hepes (pH 7.5) and 50 mM NaCl with a DNA concentration of 4.0 μM. Measurements for the T4 pol−DNA complexes were performed in 25 mM Hepes (pH 7.5), 50 mM NaCl, 1 mM DTT, 0.5 mM EDTA, and 1.0 μM DNA (p/t or p DNA). In experiments with ds and ss DNA, 2.0 and 3.0 μM T4 pol was used, respectively. In nonhydrolyzable DNA experiments, the same buffer conditions were utilized with 1.0 μM DNA and 4.0 μM T4 pol. In ds DNA experiments, Mg^{2+} was added to the samples to generate samples with 0, 0.1, 1, and 15 mM $MgCl_2$.

Titrations of dNTPs into T4 Pol−DNA Complexes. The excitation wavelength was 310 nm, and the emission was collected at 365 nm. For all four experiments, 0.5 μM DNA and 1.0 μM T4 pol were used. Three microliter additions of high-concentration nucleotide solutions were added for each titration point, spanning the final nucleotide concentration range between 7.5 μM and 6.5 mM. The fluorescence-intensity profiles were fit using a transform in Sigmaplot 4.1 (Jandel Scientific) as a sum of one and/or two independent binding equilibria (*21*).

Determination of the Fractional Populations of T4 Pol in the Exonuclease and Polymerase Sites from the Comparison of Steady-State and Time-Resolved Fluorescence Data. Determination of changes in fractional populations associated with fluorescence quenching events is often very difficult. However, in the case of the ligand-induced quenching of the 2AP hyperfluorescent state, rigorous comparison of steady-state and time-resolved fluorescence data revealed a completely "static" mechanism associated with almost all of the observed fluorescence quenching events. In a static fluorescence quenching event, the fluorescence steady-state intensities are altered, but the fluorescence lifetimes are absolutely identical (*25*). These types of fluorescence quenching events can be modeled as an equilibrium between

a fluorescent state and a "dark state" which may be excited but does not emit fluorescence. To obtain fractional populations associated with the polymerase and exonuclease sites, a "reference state", which is associated with a 100% fluorescent signal in one (of the two) sites, is required. Fortunately, for T4 pol, such a reference state exists, in that binding of ss primers are thought to be 100% localized to the exonuclease site.

In this paper, rigorous comparisons are made between steady-state fluorescence signals and time-resolved fluorescence signals from identical samples. The measured steady-state fluorescence (F_{SS}) is related to the time-resolved fluorescence (F_{TR}) with

$$F_{SS} = \int_0^\infty F_{TR}(t)\, dt \text{ where } F_{TR}(t) = \sum_i \alpha_i e^{-t/\tau_i} \quad (1)$$

and α_i is the fractional amplitude of the ith lifetime (τ_i). Carrying out this integration reveals that the steady-state fluorescence signal is related to the time-resolved fluorescence through a summation of α and τ products ($F_{SS} = \sum_i \alpha_i \tau_i$). In the majority of cases in this study, differing total intensities with identical fluorescence lifetimes are observed (e.g., Figure 3). With all τ_i between samples being identical, the amplitude component α between the samples must be the origin of the differences in the observed steady-state fluorescence intensities. Using the data in Figure 3 as a specific example, α_{SS}(single stranded) > α_{SS}(AP-C, double-stranded terminal mispair) > α_{SS}(AP-T, correctly base-paired primer terminus). The preexponential α factor is actually composed of a product of a number of terms:

$$\alpha_i = \epsilon_i(\lambda_{ex})(C_i)\mathrm{fl}_i(\lambda_{em})\mathrm{Instr}(\lambda_{ex},\lambda_{em})k^i_{Rad} \quad (2)$$

where ϵ_i is the extinction coefficient of the ith component, C_i is the fractional concentration of the ith T4 pol−DNA complex, $\mathrm{fl}_i(\lambda_{em})$ is the fluorescence emission spectrum of component i, $\mathrm{Instr}(\lambda_{ex},\lambda_{em})$ is the instrumental response, and k^i_{Rad} is the fluorescence radiative rate of component i. Since all p/t complexes have been collected under identical instrumental conditions, $\mathrm{Instr}(\lambda_{ex},\lambda_{em})$ effects can be eliminated. Also, full steady-state emission spectra comparisons reveal identical emission spectral shapes between the three bound complexes, eliminating the common $\mathrm{fl}_i(\lambda_{em})$ terms. Differences in k^i_{Rad} can be eliminated using the fact that the measured lifetimes are all identical and

$$\tau_i = \frac{1}{k^i_{Rad} + \sum_j k_{non-Rad}} \quad (3)$$

The only possibility of τ_i being the same and k^i_{Rad} for all three complexes being different would be for each to have experienced exactly compensating effects (Δ): $k^i_{Rad} \Rightarrow k^i_{Rad} + \Delta$ and $k^i_{non-Rad} \Rightarrow k^i_{non-Rad} - \Delta$. While this is possible, it is extremely unlikely that all three of the different p/t complexes studied experienced such a perfect "lifetime compensation". Canceling all of these terms yields the following relationships:

$$(\epsilon_{single-stranded})(C_{single-stranded}) > (\epsilon_{AP-C})(C_{AP-C}) > (\epsilon_{AP-T})(C_{AP-T}) \quad (4)$$

Table 1: Partitioning of 2AP at the 3′-Primer Terminus in a T4 Pol−DNA Complex into a Hyperfluorescent Exonuclease and Quenched Polymerase Site (without Mg^{2+})

complex	fraction of DNA in the exonuclease site (Exo_L)	fraction of DNA in the polymerase site (Pol_D)
WT−ss DNA	1.0	0.0
WT−ds AP-C	0.84	0.16
WT−ds AP-T	0.64	0.36
exo$^-$−AP-T[a]	0.30	0.70
exo$^-$−AP-C[a]	0.58	0.42
exo$^-$−ss DNA	0.71[b]	0.0
L412M−AP-T	0.39	0.61
L412M−AP-C	0.70	0.30
L412M−ss DNA	0.76[b]	0.0

[a] D112A/E114A exonuclease-deficient mutant. [b] Remaining fractional population associated with a dark exonuclease state (see the text). Assumptions required for the percentage partitioning assignments can be found in Methods.

To completely differentiate extinction coefficient changes from concentration changes, careful absorbance spectra were compared and found to be identical. In addition, a variety of biochemical tests were performed (described in the Results), which would be predicted to alter populations (but not extinction coefficients) via mass action effects, and found to be consistent with population shifts as the dominant mechanism associated with the static quenching observed in this system.

In those cases where a change in fluorescence lifetime was observed (e.g., low-affinity Mg^{2+} sites), individual populations were resolved by comparison of each of the individual lifetime amplitudes, using the time-resolved ss DNA signal, as a 100% exonuclease reference state. Hence, the major assumption associated with the determination of the fractional populations in Table 1 involves using the WT ss DNA signal to represent a 100% bound exonuclease site. For Table 4, the 100% exonuclease site assumption is required (for ss DNA); in addition, assignment of the increased amplitude of the shortest lifetime component at high Mg^{2+} concentrations to a polymerase emitting state or a second exonuclease site is required. If future work were to show the 100% ss bound state is distributed partially between the exonuclease and polymerase sites, then all of the population percentages presented in Tables 1 and 4 would need to be scaled down by this same factor. Similarly, Mg^{2+} titration data reveal the formation of a dark exonuclease state in the presence of millimolar Mg^{2+}. If this state were found to be populated in the absence of Mg^{2+}, then the partitioning values in Table 1 would need to be scaled down by this amount.

RESULTS

Determination of the Positional Dependence of the Fluorescence Enhancement of 2AP in the T4 Pol−DNA Complex. A large enhancement of 2AP fluorescence is found during the binding of T4 pol to p/t DNA when 2AP is located at the primer terminus (*11*). To determine the location-dependent sensitivity of this response, a series of site-specific 2AP primer−templates were prepared. An enhancement of the fluorescence intensity was observed when 2AP was located at only three sites (Figure 2). These positions were the primer terminus, 2AP across from the primer terminus on the template strand, and the template base preceding the primer terminus. The fluorescence emission spectrum

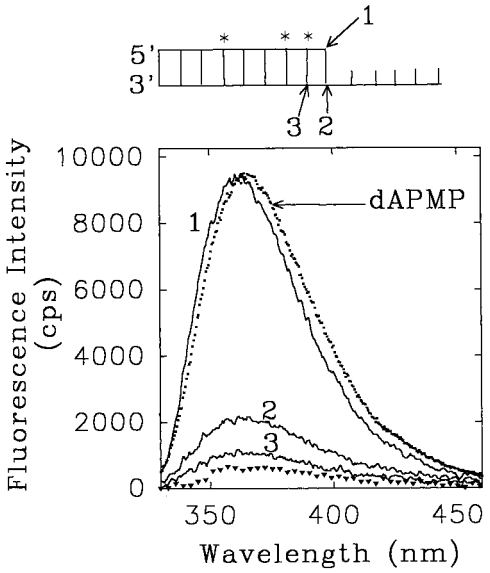

FIGURE 2: Positional dependence of 2AP fluorescence intensity enhancement in the T4 pol−p/t DNA complex. The representative 2AP fluorescence emission spectrum in free DNA (▼) is dramatically enhanced when it is bound by T4 DNA polymerase (in the absence of Mg^{2+}) when 2AP is site-specifically placed at the primer 3′-end (spectrum 1), and to a lesser extent when 2AP is positioned in the template strand directly across from the primer terminus (spectrum 2) and the template strand one base upstream (spectrum 3) from the primer terminus. Site-specific placement of 2AP at the $n - 1$, $n - 2$, and $n - 5$ positions (where n = the primer strand 3′-terminus; refer to p/t schematic) revealed no fluorescence enhancement upon T4 pol binding, indicating the extreme positional sensitivity of this enhancement. The emission spectrum of 100 nM 2-aminopurine monophosphate (dAPMP, ■) is shown to demonstrate the 5 nm shift between the bound complex and free dAPMP. The excitation wavelength was 310 nm. Reaction components are 200 nM p/t, 800 nM T4 pol, and 0.5 mM EDTA, 25 mM Hepes (pH 7.5), and 50 mM NaCl.

maxima for 2AP in these three enhanced locations are all shifted 5 nm (to shorter wavelengths) with respect to that of dAPMP (Figure 2). Interestingly, the fluorescence intensity of 2AP at the penultimate primer position ($n - 1$) was not increased when the p/t was bound by T4 pol.

Equilibrium Partitioning of DNA between the Exonuclease and Polymerase Sites in the Absence of Mg^{2+}. To determine if 2AP fluorescence is sensitive to differences in the T4 pol active sites, experiments were performed using conditions which shift the equilibrium of the p/t between the polymerase and exonuclease sites. Fluorescence of 2AP at primer 3′-ends was measured for T4 pol−DNA complexes using DNA substrates that are good substrates for polymerase activity (p/t with correct 2AP-T base pairs) and that are good substrates for exonuclease activity (single-stranded DNA and p/t with 2AP mispairs). Partitioning of primer 3′-ends between polymerase and exonuclease active sites was also altered by addition of the next nucleotides and by mutations to T4 pol that shift the partitioning to the polymerase site (L412M) and that "knock out" exonuclease activity (D112A/E114A). These experiments were performed with non-phosphorothioate DNA in the absence of catalytic Mg^{2+} ions.

The binding of WT T4 pol to correct pair, mispair, and ss DNA sequences is shown in Figure 3 (upper panel). The steady-state fluorescence intensity of the single-stranded and terminally mispaired complexes is greater than that for complexes containing correctly paired primer 3′-terminus

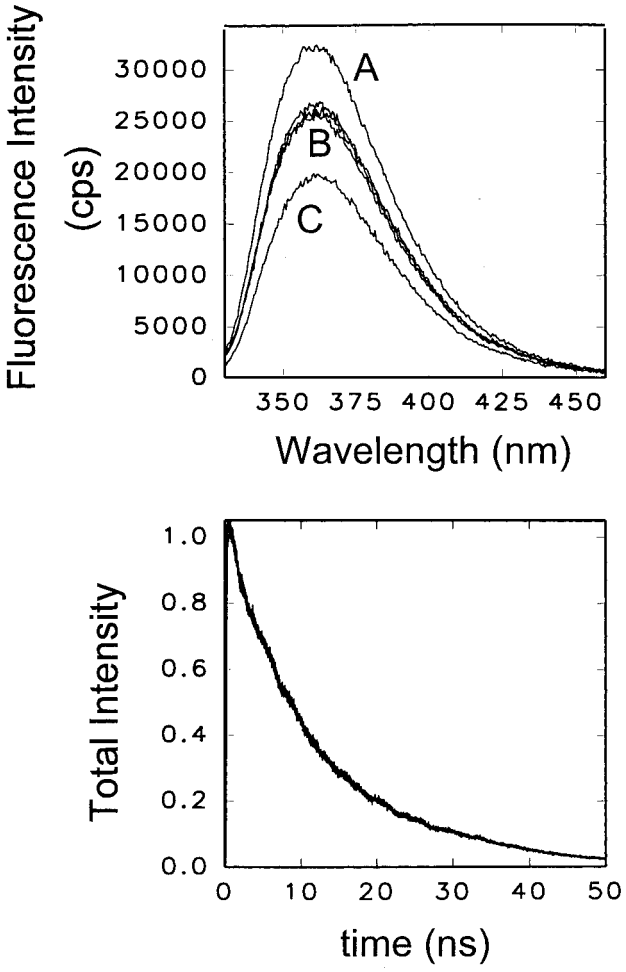

FIGURE 3: Direct comparison of the steady-state fluorescence properties (upper panel) and time-resolved fluorescence properties (lower panel) of WT T4 pol bound to DNA with 2AP at the primer terminus. (Upper panel) Steady-state emission spectra (excitation at 317 nm) of T4 pol−DNA complexes with (A) single-stranded DNA, (B) AP-A, AP-C, and AP-G mispairs, and (C) correct base pair AP-T DNA. (Lower panel) Overlapping time-resolved fluorescence decays and fits for all five samples. Steady-state experiments were performed with 0.5 μM DNA and 2.0 μM T4 pol. Fluorescence lifetime studies (excitation at 317 nm and emission at 370 nm) were performed with 1.0 μM DNA and 4.0 μM T4 pol. Both studies were performed in 0.5 mM EDTA, 25 mM Hepes (pH 7.5), and 50 mM NaCl. The DNA sequences (apart from the p/t end) are given in Materials.

DNA. Time-resolved fluorescence-intensity experiments investigated the basis for the observed differences in the steady-state intensity (Figure 3, lower panel). These experiments reveal that the decay of the fluorescence intensity is essentially identical for all of the bound complexes. Data of this type (i.e., altered steady-state intensities with identical lifetimes) are indicative of the fluorescent 2AP primer terminus in equilibrium with at least two protein conformational states, one which is hyperfluorescent and another conformation which is spectroscopically dark (i.e., does not fluoresce).

All experiments were performed under saturating protein concentrations so that small changes in K_d do not cause any change in the total population of the bound state. The measured steady-state fluorescence differences obtained in Figure 3 (upper panel), when combined with the lifetime data of Figure 3 (lower panel), require that either the primer−template is shifting between two distinct states or the

extinction coefficient of the 2AP base is altered in these various states. No measurable absorbance differences, however, were found in any of the above samples. The ss−ds hypochromic effect was already compensated for in the sample preparation. These findings suggest that altered absorption properties are not responsible for the observed steady-state fluorescence intensity differences.

Given the above logic, the simplest explanation for the observed steady-state fluorescence differences is that at least two species are present in the bound T4 pol−DNA complexes. The 2AP at the primer terminus bound at one protein site is absolutely dark and does not emit, while the primer terminus at the other site has a fluorescence which is greatly enhanced. Since the exonuclease site of T4 DNA polymerase has been shown to be too small to bind ds DNA (*5*), differences in intensity between T4 pol−ss DNA and T4 pol−ds DNA complexes should reflect the population distribution of primer ends between a single-stranded state at the exonuclease site and a double-stranded state at the polymerase site. Although it is possible that a significant population of p/t DNA could be bound at an (as yet) uncharacterized binding site, a working hypothesis for the dark state will simply be the polymerase site. A variety of additional data will be described, all consistent with this assignment.

Changes in steady-state intensity can be combined with changes in the fluorescence lifetimes to calculate fractional populations of the primer ends between the two states (see Methods). When the signal for a WT T4 pol−ss DNA complex is set to represent a population where 100% of the 2AP primer ends are bound at the exonuclease active site, the fraction of primer ends bound in the exonuclease and polymerase sites can be calculated for other complexes (Table 1). The fraction of AP−DNA bound at the exonuclease site decreases in the order single-stranded (100% exo site, by definition) → AP-C mispair (84% exo site) → AP-T (64% exo site). In this model, differences in fluorescence intensities of T4 pol−DNA complexes are interpreted as differences in populations of AP-labeled primer ends bound at the exonuclease active site to form hyperfluorescent complexes and bound at the polymerase site to form spectroscopically dark complexes. It should be emphasized that this result is the partitioning between the exonuclease and polymerase sites in the absence of Mg^{2+}. In the presence of Mg^{2+}, this partitioning will shift further toward the polymerase site (see below).

To further strengthen this initial assignment of the hyperfluorescent site being associated with the exonuclease site, and the dark site associated with the polymerase site, two T4 polymerase mutants were examined: D112A/E114A and L412M. D112A/E114A is an exonuclease knock-out mutant, wherein two essential Mg^{2+} chelating residues have been replaced with alanine so that its exonuclease activity is reduced by about 1000-fold relative to that of WT (*15*). L412M has a normal exonuclease active site but has had a single residue changed in the proposed polymerase-switching domain (near palm domain in Figure 1) which reduces the concentration of the primer strand in the exonuclease site (*26*, *27*). As described above, steady-state and time-resolved fluorescence experiments were performed at identical reagent concentrations (Figure 4). Again, as observed with the sequence-dependent experiments, steady-state fluorescence-

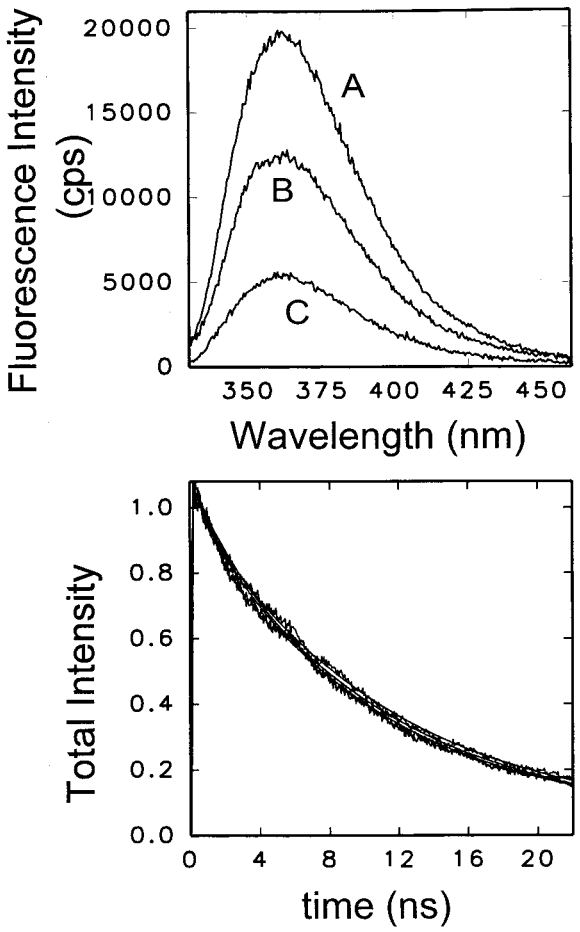

FIGURE 4: Direct comparison of the steady-state fluorescence properties (upper panel) and time-resolved fluorescence properties (lower panel) of WT and two mutant T4 pols bound to DNA with 2AP at the primer terminus. (Upper panel) Steady-state emission spectra of (A) WT, (B) mutant L412M, and (C) exonuclease-deficient mutant D112A/E114A T4 pols. (Lower panel) Overlapping time-resolved fluorescence decays and fits for the bound complexes of all three samples. Steady-state experiments were performed with 0.5 μM DNA and 2.0 μM T4 pol. Fluorescence lifetime studies (excitation at 317 nm and emission at 370 nm) were performed with 1.0 μM DNA and 4.0 μM T4 pol. Buffer conditions were identical to those of Figure 3.

intensity differences are observed (Figure 4, upper panel) with no significant changes in the observed fluorescence lifetimes (Figure 4, lower panel). Fractional populations in the polymerase and exonuclease sites can be estimated from these data (as described above) and are listed in Table 1. The fraction of AP-T primer within the exonuclease site is reduced relative to WT enzyme by an additional 25 and 34% for L412M and D112A/E114A DNA polymerases, respectively. The correlation of lower fluorescence and decreased exonuclease activity supports our initial spectroscopic assignment of a hyperfluorescent exonuclease site.

Studies performed on mismatched p/t ends were also performed with the WT and mutant enzymes. With mismatched p/t ends, one would expect an increase in the proportion of primer ends in the exonuclease site relative to the polymerase site. A clear shift in population of this type is observed (Table 1). The mispair AP-C caused an additional 20, 28, and 29% of the p/t ends to migrate to the exonuclease site in the wild type and D112A/E114A and L412M mutants, respectively (Table 1). Again, these results

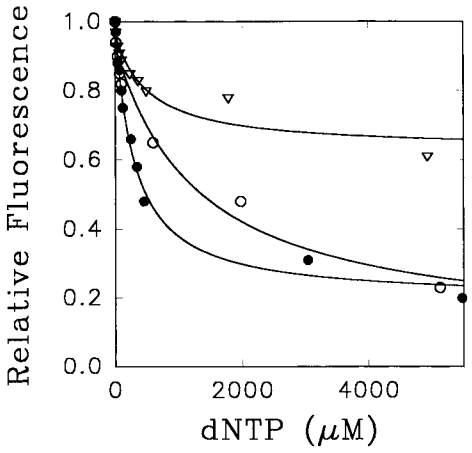

FIGURE 5: Changes in steady-state fluorescence of 2AP (at the primer terminus) in WT T4 pol bound complexes upon addition of deoxynucleotides in the absence of Mg^{2+}: T4 pol−ss DNA (17mer) complex titrated with dATP (▽, $K_d \approx 0.8 \pm 0.5$ mM); T4 pol−ds DNA complex (17mer−30mer) titrated with an incorrect next nucleotide, dATP (○, $K_d \approx 2.0 \pm 0.6$ mM); and T4 pol−ds DNA complex (17mer−30mer) titrated with correct next nucleotide, dTTP (●, $K_d \approx 0.31 \pm 0.05$ mM). Very approximate K_ds were obtained from nonlinear fits of the data using a single saturation binding isotherm (smooth lines through the data); actual binding may be more complex. The concentrations of T4 pol and DNA used in each experiment were 1.0 and 0.5 μM, respectively.

are consistent with the initial spectroscopic assignment of the light and dark fluorescence states to exonuclease and polymerase states, respectively.

Comparisons were made between the absolute fluorescence intensities associated with WT and mutant complexes bound to ss DNA. Both mutant T4 pol−ss DNA complexes have less fluorescence intensity than the WT complex. In all of these cases, however, 100% binding of ss DNA within the exonuclease site would be expected. If this proposal is correct, then these experiments indicate the presence of an additional state within the exonuclease site which can also be spectroscopically dark (see Table 1). Because the hyperfluorescent complexes in all three of these ss DNA complexes (WT and mutants) have identical lifetimes, only population shifts seem to be responsible for the measured intensity differences. Pre-steady-state kinetic studies (*12*) and additional experiments (described below) will provide evidence for the presence of a dark state within the exonuclease active site.

Another method for altering the polymerase:exonuclease ratio is by the addition of deoxynucleoside triphosphates via mass action effects. Deoxynucleoside triphosphates increase the relative concentration of p/t within the polymerase active site. Given the spectroscopic assignment (described above), addition of dNTPs should result in a decrease in fluorescence intensity, as the p/t equilibrium switches from the hyperfluorescent exonuclease site and is transferred to the polymerase site. dNTP addition experiments were performed using the next correct dNTP, incorrect dNTPs, and dNTPs with single-stranded DNA as a control (Figure 5). In all experiments, addition of nucleotides resulted in a saturable decrease of fluorescence intensity. In the absence of Mg^{2+}, the binding of the correct dNTPs was found to have an affinity nearly 1 order of magnitude tighter than the binding constant for incorrect nucleotide. The sensitivity of the spectroscopic signal for discriminating between correct and incorrect next nucleotides further supports the idea that this fluorescence quench is not related to some nonspecific nucleotide effect.

A smaller quenching is observed for dNTP binding to ss DNA, which should not be capable of switching between the exonuclease and the polymerase sites (Figure 5). Crystallographic (*4*) and NMR (*28*) studies have revealed, however, that dNTPs can also bind into the channel in which the exonuclease binds the ss primer, thereby competing for the exonuclease active site. This effect would appear as a small amplitude (relative to ds DNA) quenching term upon titration of dNTPs into ss T4 pol−DNA complexes. Such an effect is indeed observed for dATP titrated into WT ss DNA complexes (Figure 5). Alternatively, a small population of ss DNA molecules may be bound in the polymerase active center.

The fraction of species switched from the exonuclease to the polymerase active site at specific nucleotide concentrations reveals a dNTP-dependent increase in the fraction of AP−DNA bound in the dark polymerase active site. In the absence of any dNTPs, 36% of the p/t ends are in the polymerase site. Addition of the correct next base dNTP increases this percentage to 60% (at 0.5 mM) and finally to 73% at 5.3 mM dNTP. Binding of the incorrect dNTP shifts the equilibrium more slowly, but eventually at high dNTP concentrations results in approximately the same magnitude shift in population (Figure 5).

Binding of Mg^{2+} to the T4 Pol−ss and −ds DNA Complexes. All previous Mg^{2+} binding studies to DNA polymerases have been performed in the absence of ss or ds DNA due to exonucleolytic hydrolysis of the DNA. To eliminate this complication, hydrolysis resistant AP−DNA was prepared with an S_p phosphorothioate linkage to the phosphate of the 2AP 3′-primer terminal base (see Methods). This phosphorothioate linkage prevents hydrolysis during the time course of our experiments, allowing a direct spectroscopic examination of Mg^{2+} binding in the presence of DNA. Because the 3′ → 5′ exonuclease of T4 pol can also function as a blunt-end exonuclease, template strand DNA with this same S_p phosphorothioate linkage (at the 3′-end) was also required. This "doubly resistant" 2AP-containing DNA was found to be capable of remaining intact during the entire time course (∼a few hours) of a Mg^{2+} titration experiment (see Methods).

Addition of Mg^{2+} resulted in an overall decrease in the fluorescence intensity of 2AP at a primer terminus in WT and mutant T4 pols bound to ds DNA (Figure 6A) and ss DNA (Figure 6B). As expected, mutation of putative divalent metal coordinating residues, D112, E114, D219, and D324, greatly affected the shapes (and phases) associated with Mg^{2+} binding. Nonlinear fitting of these binding isotherms was performed using both a single dissociation constant and two distinct dissociation constants (Table 2), and the goodness of fit was quantitated using a χ^2 criterion (i.e., sums of the squares of the residuals). For most of the cases, the presence of two binding transitions was apparent after visual inspection of the data. The two borderline multiphasic cases are D324A and D112A/E114A binding to ds DNA (Figure 6A). For these cases, the use of two distinct dissociation constants improved the quality of the fit using an *F*-test criteria (*24*), and confidence levels (for accepting the two K_d solutions as better than one) were at the 90 and

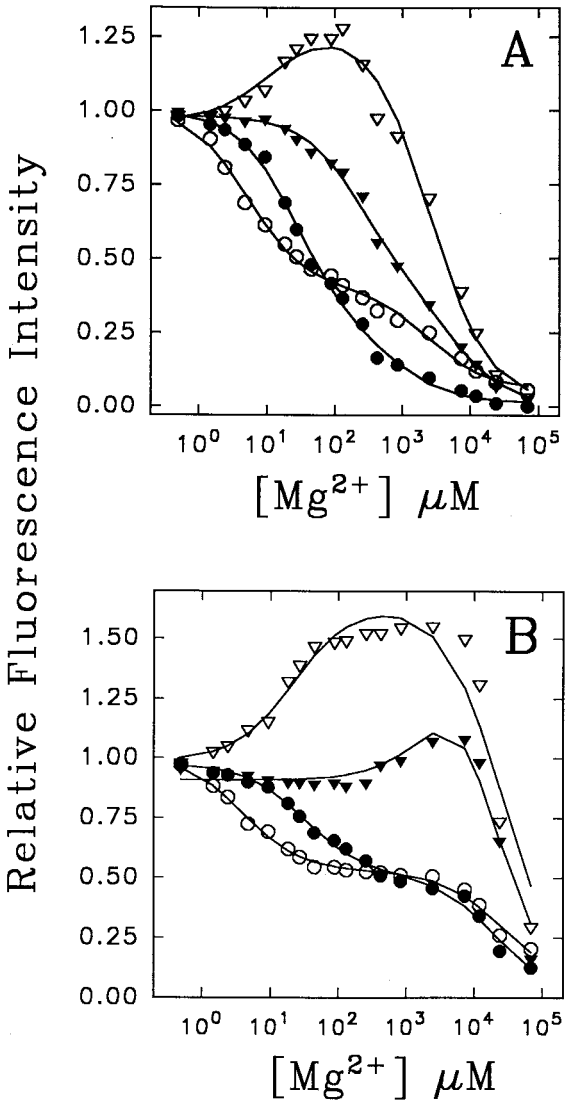

FIGURE 6: Equilibrium binding of Mg^{2+} to T4 pol bound to ds DNA (A) and ss DNA (B). 2AP is located at the 3′-primer terminus (see Materials for the sequence). The 3′-ends of both the primer and template DNA were synthesized with hydrolysis resistant 3′ S_p enantiomer phosphorothioate linkages (see Methods), allowing these titrations to be performed without the complication of DNA degradation. (A) T4 pol complexed with double-stranded DNA (17mer−30mer): WT (○), D324A (●), D112A/E114A (▼), and D219A (▽). (B) T4 pol complexed with the ss 17mer primer: WT (○), D324A (●), D112A/E114A (▼), and D219A (▽). Experimental conditions were 1.5 μM T4 pol, 250 nM DNA, 25 mM Hepes (pH 7.5), 50 mM NaCl, and 1 mM DTT. Full spectra were obtained within 5 min after each Mg^{2+} addition. Smooth lines through the data represent nonlinear fits using two independent binding phase sites (as described in Methods). Recovered dissociation constants for Mg^{2+} binding are reported in Table 2.

67% levels for D112A/E114A and D324A, respectively.

The dominant biphasic transitions observed for Mg^{2+} binding are characterized by a high-affinity micromolar K_d and a low-affinity millimolar K_d (see Table 2). Since the hyperfluorescent signal is associated with 2AP at the primer terminus in the exonuclease active site, and the polymerase site is highly quenched, these K_ds may reflect both direct binding of Mg^{2+} within the exonuclease site and any change in equilibrium between polymerase and exonuclease sites which are Mg^{2+}-dependent. High-affinity (micromolar) binding constants are weaker for exonuclease-deficient T4 pol mutant−DNA complexes than for WT T4 pol−DNA complexes, while low-affinity (millimolar) binding constants are essentially unchanged. The high-affinity Mg^{2+} ion binding is similar for complexes formed with both ss and ds DNA. The second, low-affinity (millimolar) binding transition reveals that Mg^{2+} binds T4 pol−ss DNA complexes approximately 10-fold more weakly than T4 pol−ds DNA complexes. Time-resolved anisotropy experiments (see below) verified that at higher Mg^{2+} concentrations the WT and D324A mutant T4 pol−DNA complexes were not dissociating due to nonspecific ionic strength effects. A small amount of T4 pol dissociation was observed above 5 mM $MgCl_2$ for complexes containing the D219A and D112A/E114A mutants.

Table 2: High- and Low-Affinity Dissociation Constants for Mg^{2+} Binding to T4 Pol DNA Complexes

enzyme	K_{d1} (μM)	K_{d2} (mM)
Complexes Containing ds DNA (17mer−30mer)		
WT	5.1 ± 0.6	2.5 ± 0.7
D324A[a]	27 ± 5.0	0.8 ± 0.5
D219A	11 ± 7.0	2.5 ± 0.5[b]
D112A/E114A[a]	235 ± 60	5.4 ± 2.5[b]
Complexes Containing ss DNA (17mer)		
WT	3.0 ± 0.5	26 ± 7.0
D324A	32 ± 6.0	21 ± 7.0
D219A	22 ± 11	27 ± 12[b]
D112A/E114A	900 ± 390	19[b]

[a] These two borderline two-site cases have single K_d solutions of 602 ± 80 μM for D112A/E114A and 49 ± 5 μM for D324A. [b] In these experiments, some dissociation of T4 pol from the DNA occurs at high Mg^{2+} concentrations, complicating the determination of the lower-affinity sites.

Time-Resolved Fluorescence Studies of 2AP within T4 Polymerase Phosphorothioate−DNA Complexes and Determination of the Partitioning between Pol and Exo Sites over a Range of Mg^{2+} Concentrations. To understand the dominant mechanism responsible for the change in steady-state fluorescence associated with the measured Mg^{2+} binding titrations, time-resolved fluorescence measurements were performed. 2AP fluorescence (as dAPMP) is insensitive to quenching by Mg^{2+} ions at concentrations up to 400 mM (*3*), indicating that the observed quench is not related to some intrinsic property of 2AP fluorescence. Mg^{2+} titrations of the ss and ds DNA in the absence of T4 pol resulted in no observed quenching (data not shown).

Figure 7 (upper panel) shows the time-resolved total intensity (fluorescence lifetime) and time-resolved anisotropy (lower panel) for the WT T4 pol−ds DNA complex at four Mg^{2+} concentrations. The total-intensity decay shows that the fluorescence lifetime of 2AP within the T4 pol−DNA complex remains the same between 0 and 0.1 mM Mg^{2+} but decreases above 0.1 mM (Figure 7, upper panel, and Table 3). Similarly, the rotational properties of the primer terminus are also invariant between 0 and 0.1 mM MgCl, but an increasing amplitude for rapid motion occurs above 0.1 mM (Figure 7, lower panel).

Titration of the high-affinity Mg^{2+} binding site (between 0 and 100 μM Mg^{2+}) in the WT T4 pol−DNA ds complex results in a large (≈60%) quench in the steady-state fluorescence intensity (Figure 6A,B). Remarkably, the time-resolved fluorescence lifetime(s) and mean lifetime ($\langle\tau\rangle$) are invariant over this concentration range (Table 3 and Figure

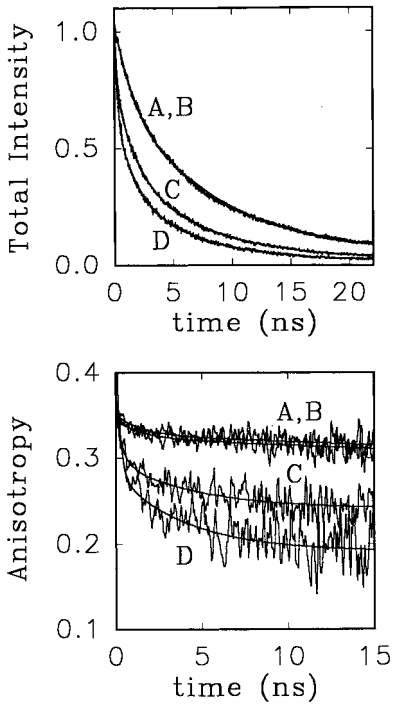

FIGURE 7: Time-resolved fluorescence total intensity (upper panel) and rotational mobility (lower panel) of the 3′-primer terminus of p/t DNA when bound by WT T4 pol as a function of increasing Mg^{2+} concentration. **(**Upper panel) Time-resolved fluorescence decays of 2AP at the primer terminus of WT T4 bound double-stranded DNA at 0.0 (A), 0.1 (B), 1.0 (C), and 15.0 mM (D) $MgCl_2$. **(**Lower panel) Rotational mobility of 2AP at the 3′-primer terminus of WT T4 bound to double-stranded DNA at 0.0 (A), 0.1 (B), 1.0 (C), and 15.0 mM (D) $MgCl_2$. Experiments were performed using 1.0 μM nonhydrolyzable (see Methods) p/t DNA and 4.0 μM T4 polymerase; the excitation wavelength was 317 nm and the emission wavelength 365 nm.

Table 3: Fluorescence Lifetimes of 2AP at the 3′-Primer Terminus of ss DNA (17mer) and ds DNA (17mer−30mer) Bound to T4 Pol at Increasing Mg^{2+} Concentrations[a]

DNA type	$[Mg^{2+}]$ (mM)	α_1	τ_1 (±0.07)	α_2	τ_2 (±0.2)	α_3	τ_3 (±0.2)	$\langle\tau\rangle$
ss	0.0	0.08	0.161	0.38	2.2	0.54	10.7	6.6
ss	8.0	0.20	0.283	0.46	2.4	0.34	9.8	4.4
ds	0.0	0.17	0.088	0.28	1.7	0.55	9.4	5.7
ds	0.1	0.11	0.128	0.29	1.6	0.60	9.3	6.1
ds	1.0	0.47	0.129	0.30	2.0	0.23	9.2	2.8
ds	15.0	0.56	0.137	0.26	1.9	0.18	8.1	2.0

[a] All τ values are in nanoseconds.

7, upper panel), indicating a 100% static quenching mechanism associated with the high-affinity Mg^{2+} site(s). Since both the T4 pol−ds and −ss DNA complexes experience approximately an equal decrease in steady-state intensity, the dark state responsible for the majority of this quenching must be accessible to both ds and ss DNA complexes. These observations are most consistent with a Mg^{2+}-induced dark state at the exonuclease site. An initial hint of the existence of an exonuclease dark state was obtained from the comparison of WT and mutant ss DNA bound complexes (Table 1). The Mg^{2+}-induced dark state appears to be generated both by direct binding in the exo$^-$ site (e.g., WT and L412M) and by alterations in the exo$^-$ site caused by Mg^{2+} binding predominantly in the polymerase site (e.g., D412A/E114A).

Unlike that for the high-affinity sites, filling up the low-affinity Mg^{2+} sites (1−15 mM Mg^{2+}) in the T4 pol−ds DNA complexes alters the fluorescence lifetime(s) of 2AP, decreasing the mean lifetime from 6.1 to 2.0 ns (Table 3). Examination of the full time-resolved fluorescence response, however, reveals that the decrease in mean $\langle\tau\rangle$ is not associated with a significant change in any single lifetime, but rather a decrease in the amplitude of the long lifetime term (60 → 18%) and an increase in the amplitude of the shortest lifetime term (11 → 56%), the middle lifetime amplitude being invariant at approximately 30%. Similar to the titration of the high-affinity site, the steady-state intensity changes of the millimolar affinity sites are dominated more by changes in populations than by changes in lifetimes.

Table 4: Partitioning of 2AP at the 3′-Primer Terminus in Phosphorothioate-Protected ss DNA (17mer) and ds DNA (17mer−30mer) When Bound by T4 Pol

DNA type	$[Mg^{2+}]$ (mM)	total quench[a] (%)	dynamic quench[a] (%)	static quench[a] (%)	Exo_L	Exo_D	Pol_L	Pol_D
ss	0.0	−	−	−	1.0	−	−	−
ss	8.0	55	33	22	0.78	0.22	−	−
ds	0.0	60	14	46	0.42	−	0.04	0.54
ds	0.1	82	8	74	0.17	0.16	0.02	0.65
ds	1.0	88	58	30	0.13	0.17	0.06	0.64
ds	15.0	95	70	25	0.05	0.17	0.04	0.74

[a] Mean lifetimes utilized to decompose the measured steady-state quenching into static and dynamic quenching components. All quenching is reported relative to the steady-state fluorescence intensity and mean lifetime for ss DNA complexes at 0 mm $MgCl_2$.

Comparison of the lifetimes associated with ss and ds DNA bound complexes reveals that the ds DNA bound complexes have a much larger fraction associated with the shortest lifetime component at high Mg^{2+} concentrations (Table 3). For instance, at 8 mM Mg^{2+}, a 20% amplitude is associated with the short lifetime component in ss DNA, whereas a 47% amplitude component exists in ds DNA at 1 mM Mg^{2+}. If the emitted fluorescence for ds and ss DNA complexes were both from 2AP located solely within the exonuclease site, the lifetimes and relative amplitudes for ss and ds DNA would be the same (as was found in the absence of Mg^{2+}; lower panels of Figures 3 and 4). The ds DNA complex, however, has a much larger fraction associated with the shortest lifetime species. This suggests that a portion of this short lifetime species comes from a state which is inaccessible to ss DNA but present in ds DNA complexes. A plausible state for this fluorescence emission is a highly quenched (but not totally dark) polymerase site. At high Mg^{2+} concentrations (≥1 mM $MgCl_2$), the amplitudes associated with the two longest 2AP fluorescence lifetimes for ss and ds DNA complexes are essentially the same, indicating that the emission from the putative polymerase state has no significantly populated long-lived components. Within this model framework, the approximate fractions of all of the protein−DNA populations (Exo_L, Exo_D, Pol_D, and Pol_L) as a function of Mg^{2+} concentration can be calculated (Table 4). It should be emphasized that the populations determined as a function of Mg^{2+} concentration (Table 4) are more model-dependent than those recovered in the absence of Mg^{2+}, where the system exhibits nearly perfect two-state behavior (Table 1).

Change in the Rotational Mobility of the Primer Terminus upon Addition of Mg^{2+}. Time-resolved anisotropy studies

were performed to investigate the motional properties of the p/t terminus in the high-affinity and low-affinity Mg^{2+} binding regimes (Figure 7, lower panel). This type of experiment determines the motional state of the primer terminus within the T4 pol−DNA complex. Rapid decay of the time-resolved anisotropy is indicative of a fast "local" motion of 2AP within the binding site(s). The global tumbling of the entire T4 pol−DNA complex has a correlation time of approximately 100 ns (*11*); hence, all of the fast motion observed in Figure 7 (lower panel) is associated with local rotational freedom of the 2AP primer end within the exonuclease and polymerase binding sites. The motion of the 2AP in the absence of Mg^{2+} is very restricted, with only a small amount (≈5%) of rapid, local motion with a correlation time of 1.5 ns (Figure 7, A and B in the lower panel). At Mg^{2+} concentrations up to 0.1 mM, the rotational properties of 2AP within the T4 pol−DNA complex remain the same. Above 0.1 mM Mg^{2+}, the fractional component of the rapid local motion of the primer terminus increases dramatically, to almost 50% total depolarization.

DISCUSSION

Photophysical Origin of the 2-Aminopurine Hyperfluorescent State. In the absence of polymerase, adjacent bases, primarily the vertical base stacking partners, are the main quenching agent of 2AP fluorescence in ss and ds DNA (*3*). The simplest interpretation of the large enhancement of 2AP fluorescence at the primer terminus upon interacting with T4 pol is that the vertical base stacking component of the primer terminus is greatly decreased upon binding. By varying the location of the single 2AP site within the T4 pol−ds DNA complex, we found that the fluorescence enhancement was almost completely localized to the primer terminus, with the $n - 1$ primer position showing no fluorescence enhancement upon binding (Figure 2). When the 2AP-containing oligonucleotides were being synthesized, it was anticipated that the observed site-specific fluorescence enhancement would "map out" the single-stranded versus double-stranded "melting region" associated with pulling the p/t apart. This effect would have generated a two- to four-nucleotide "window" of fluorescence enhancement which could be observed from the primer strand. Clearly, this result was not obtained.

Examination of the structure of the ss dT_{16} bound to bacteriophage RB69 DNA polymerase provides a very simple explanation for the structural origin of the hyperfluorescent state of 2AP when it is placed at the primer terminus which is consistent with this extreme positional dependence. The RB69 DNA polymerase is 63% identical with T4 pol and hence serves as a good model for understanding structural transitions in the primer terminus of T4 pol. A surprising result from the RB69 DNA pol·dT_{16} structure was the intercalation of F123 between the two terminal bases in the exonuclease binding site (see Figure 6b in ref *2*). We propose that a similar intercalation event occurs in T4 pol, with F120 playing the same role as F123 in RB69 DNA pol. Such an intercalation event would eliminate the vertical base stacking of 2AP at the primer terminus and cause a very localized hyperfluorescent state, consistent with the observed sequence-dependent data. The lack of fluorescence enhancement at the $n - 1$ primer position indicates that complete 2AP quenching can occur with only one tightly packed base stacking partner.

This interpretation is consistent with our earlier studies of KF binding to an identical 2AP-containing primer (*22*). Binding of KF revealed only a 1.5-fold fluorescence enhancement when it was bound in the absence of Mg^{2+}. Although both KF and T4 pol probably strand-separate similar lengths of p/t and the overall structures of both exonuclease sites are similar, KF clearly lacks any intercalating amino acid at the primer terminus. At the current time, we have no explanation for the fluorescent enhancements associated with the n and $n - 1$ template positions, other than to suggest that some alteration of base stacking also occurs at these positions in the polymerase active site.

Our structural interpretation of the 2AP fluorescence enhancement utilizes the F123 intercalation observed in the crystal structure of the RB69 DNA polymerase (*2*). Hence, the binding of RB69 DNA pol to 2AP-containing primer strands would also be predicted to reveal a large fluorescence enhancement. Experiments of this type were performed, and RB69 was found to produce a large fluorescence enhancement very similar in magnitude to that of T4 polymerase, but without the concomitant 5 nm blue shift in the emission spectrum (L. J. Reha-Krantz, unpublished observations). RB69 and T4 pol are the only two DNA polymerases in which such a large 2AP-enhanced fluorescence has been observed.

Time-resolved fluorescence anisotropy studies of T4 pol−DNA reveal very little local motion of 2AP within this bound complex (see the lower panel of Figure 7). Such restricted motion would be predicted with an intercalated phenylalanine restricting local motion of the primer terminus.

A 5 nm blue shift is observed in T4 pol for the hyperfluorescent bound state (Figure 2). Blue shifts of this magnitude have been observed for 9-ethyl-2-aminopurine when it is placed in more hydrophobic solvents (*3*), consistent with a hydrophobic primer terminus environment. Examination of the region around the primer terminus in the T4 exonuclease site reveals a very hydrophobic "pocket", with Val 115, Phe 120, Phe 218, and Ise 306 surrounding the primer terminus.

Mg^{2+} Binding Properties of T4 Pol−DNA Complexes when They Are Saturated with ss and ds DNA. We report the first studies of Mg^{2+} binding to T4 DNA polymerase complexed with DNA. These studies were made possible by the synthesis of fluorescent nonhydrolyzable phosphorothioate DNA substrates. Lanthanide binding to T4 pol (in the absence of ss or ds DNA) revealed the presence of a single high-affinity site in the micromolar concentration range. Characteristic signatures of lower-affinity binding sites were noted but could not be quantitated (*29*). The most closely related divalent metal binding studies on a DNA polymerase are the EPR and NMR studies of the binding of Mn^{2+} to *Escherichia coli* DNA polymerase I (*30*). In these studies, prebinding dGTP was utilized to model WT pol I bound to p/t ds DNA, whereas prebound dTMP mimicked ss DNA. In the presence of dGTP and dTMP, WT pol I was found to have high- and low-affinity sites for Mn^{2+} of 6.7−7.8 μM and 1.8−2.6 mM, respectively. In this study, both high-affinity (5.1 μM) and low-affinity sites (2.5 mM) were also obtained, with nearly identical dissociation constants. The consistency of the 2AP spectroscopic and NMR

results further supports the use of this spectroscopic approach for monitoring binding transitions in this class of enzymes. In addition, it appears as if two affinity classes (micromolar and millimolar) of divalent binding sites might be a general property of DNA polymerases.

It should be pointed out that, for some mutants, addition of Mg^{2+} actually results in a transient fluorescence increase before a final fluorescence decrease (Figure 6; D219A). Comparison of the absolute fluorescence intensities, however, reveals that the absolute intensities of the D219A T4 pol in the absence of Mg^{2+} are 40% quenched compared to that of WT. Therefore, the fluorescence enhancement observed during the titration of the high-affinity site of D219A (Figure 6A,B) actually represents more of a "dequenching", equalizing the fluorescence intensities with that observed with the WT bound complex. Mg^{2+} binding appears to "rescue" (to some extent) the structural perturbation induced in the p/t end by the D219A amino acid substitution, making the site appear, spectroscopically, more like WT.

Examination of the exonuclease active site of T4 polymerase reveals a tight interplay of multiple carboxylates chelating two divalent metal sites (*5*). Therefore, interpretation of these biphasic isotherms (in terms of which class of Mg^{2+} binding sites is associated with a specific carboxylate group) must remain rather speculative. The >10-fold weaker binding for the high-affinity site of D112A/E114A (the exonuclease knock out), however, suggests that the high-affinity sites may be more localized to the exonuclease site. Analogous amino acid substitutions in the KF prevent divalent metal binding (*13*).

Partitioning of the T4 Pol−DNA Complexes into Polymerase and Exonuclease Sites. Evidence exists for four spectroscopically distinct states (Exo_L, Exo_D, Pol_L, and Pol_D) associated with the p/t terminus when it is bound to T4 pol in the presence of Mg^{2+}. Of these four states, the hyperfluorescent exonuclease (Exo_L) and dark polymerase (Pol_D) always represent the majority (≥80%) of all species present. The equilibrium between these four states can be altered in the following manner.

(1) DNA destabilized at the primer terminus (e.g., single-stranded, mispaired ds DNA) results in a shift from the dark polymerase state (Pol_D) to the hyperfluorescent exonuclease state (Exo_L) (Tables 1 and 4). The fraction of AP−DNA bound at the exonuclease active site in the absence of Mg^{2+} is high (≈64%), "out-competing" the polymerase site for the primer end by forming a very tightly bound complex (Figure 7, lower panel) with a locally unstacked intercalated primer terminus (Figure 2).

(2) The D112A/E114A exonuclease-deficient and L412M polymerase-switching mutants can move a significant fraction (25 and 34%, respectively) of the primer terminus from the exonuclease site (Exo_L) to the polymerase site (Pol_D) (Figure 4 and Table 1), consistent with each mutant's phenotype.

(3) Titration of dNTPs into the complex shifts the equilibrium from the hyperfluorescent exonuclease state to the dark polymerase state. This shift is considerable, such that the fraction of the primer terminus in the exonuclease active site can be decreased from 64% in the absence of dNTPs to as little as 27% at high concentrations (5 mM) of dNTP. Under all experimental conditions studied, exonuclease activity and measured fluorescence intensities are absolutely correlated, supporting the assignment of the hyperfluorescent state to the exonuclease site.

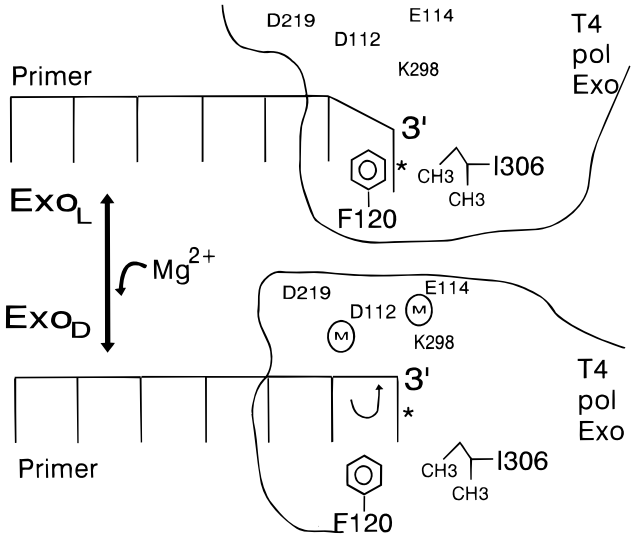

FIGURE 8: Proposed physical mechanism associated with the Mg^{2+}-induced high- and low-affinity switches in T4 pol. In the absence of Mg^{2+}, phenylalanine 120 (F120) in the exonuclease site of T4 pol intercalates into the primer terminus, causing a large fluorescence enhancement in 2AP located at the 3′-primer terminus (*). A largely hydrophobic binding pocket is proposed to stabilize the primer terminus. Upon binding of Mg^{2+} in the exonuclease site (especially at D219, D112, and E114), the phosphate backbone at the primer terminus is pulled backward as it begins to participate in the overall chelation of the bound Mg^{2+}. As the primer terminus contracts backward into the exonuclease active site, the fraction of primer termini with F120 base-intercalated decreases, causing the observed decrease in the fluorescence intensity generating the Exo_D state. This loss in intercalation energy allows the polymerase site (which is probably also binding Mg^{2+}) to more favorably compete with the exonuclease active site for primer termini, resulting in a net population shift from the exonuclease to polymerase sites. This Mg^{2+} switching model combines the structural data from ref *2* (see their Figure 7B) with the Mg^{2+}-induced spectroscopic changes observed in this work.

Possible Physical Origin of the Mg^{2+}-Induced Conformational "Switch" in T4 Pol. Mg^{2+} has two distinct effects on the equilibrium between the four T4 pol states populated at equilibrium (Table 4). During the filling of the high-affinity Mg^{2+} binding site(s) (≤100 μM $MgCl_2$), the hyperfluorescent T4 pol exonuclease state (Exo_L) shifts to both the dark exonuclease (Exo_D) and dark polymerase (Pol_D) states. Examination of the structure of the exonuclease site in the RB69 DNA pol suggests there is a possible physical origin associated with this high-affinity Mg^{2+} switch (see Figure 8; use Figure 6b of ref *2* for a three-dimensional structural viewpoint). The important amino acid residues associated with the binding of Mg^{2+} in the exonuclease site of RB69 are located on the opposite face of the primer terminus with intercalated F123. As the metal ions chelate T4 pol's D112, E114, and D219, they also coordinate with the negatively charged phosphate backbone, all located directly opposite (behind) the intercalating F120 and primer terminus. It is proposed that this Mg^{2+} binding "pulls" the primer terminus away from the intercalating F120 (Figure

8), causing the observed large Mg^{2+}-dependent quenching. The elimination of the base intercalation interaction energy from the exonuclease site, as well as any secondary binding effects (e.g., Mg^{2+}-associated p/t stabilization at the polymerase site), allows the polymerase site to compete more effectively for the primer terminus, resulting in the overall shift in the equilibrium population of primer termini from the exonuclease site to the polymerase site. This hypothetical high-affinity Mg^{2+} switch simultaneously accounts for all of the observed spectroscopic quenching data and population shifts that have been observed in this study.

Filling of the low-affinity Mg^{2+} binding site(s) ($\geq 100\ \mu M$ $MgCl_2$) reveals that the rotational dynamics associated with the primer terminus are radically altered. What was once a rigidly held primer terminus now shows significant rotational motion on the nanosecond time scale (Figure 7, lower panel, C and D). According to our model (Figure 8), this effect is due to movement of the primer terminus from the highly restrictive intercalated, hydrophobic exonuclease site to a highly quenched exonuclease and polymerase site which does not hold the primer terminus very tightly. Interestingly, it is in this low-affinity Mg^{2+} binding regime where the catalytic enzyme activity increases dramatically, with maximal activity not being reached until $\approx$6 mM Mg^{2+}. The low-affinity Mg^{2+} switch may therefore be associated with T4 pol loosening its grip on the p/t termini in a manner such that the proper geometries, water accessibilities, etc., associated with catalysis and exonuclease reactions can be realized (*31*). An absolutely rigid binding site may not be possible in this class of enzymes, due to the dual requirement of p/t switching and needing to "sense" correctly paired termini from mispaired primer termini.

The total fraction of species present in the exonuclease site decreases from 42 to 22% upon increasing Mg^{2+} from 0 to 15 mM (Figure 6 and Table 4). When one takes into account both the Mg^{2+} and dNTP effects on partitioning, the spectroscopically determined distribution of p/t between the polymerase and exonuclease sites is well within the range of populations (8−25% at exonuclease site) previously estimated from polymerase:exonuclease ratios (*26*, *32*).

In the following paper (*12*), pre-steady-state kinetic experiments are performed which provide unequivocal kinetic support for the existence of a minimum of two highly populated primer-end states on T4 pol with very different base stacking properties. In addition, the sequential pathway and rate constants connecting these various p/t conformational states are directly measured.

ACKNOWLEDGMENT

J.M.B. gratefully acknowledges Prof. Jimin Wang (Yale University, New Haven, CT) for providing graphics assistance with Figure 1.

REFERENCES

1. Freemont, P. S., Friedman, J. M., Beese, L. S., Sanderson, M. R., and Steitz, T. A. (1988) *Proc. Natl. Acad. Sci. U.S.A. 85*, 8924−8928.
2. Wang, J., Sattar, A. K. M. A., Wang, C. C., Karam, J. D., Konigsberg, W. H., and Steitz, T. A. (1997) *Cell 89*, 1087−1099.
3. Ward, D. C., Reich, E., and Stryer, L. (1969) *J. Biol. Chem. 244*, 1228−1237.
4. Beese, L. S., Derbyshire, V., and Steitz, T. A. (1993) *Science 260*, 352−355.
5. Wang, J., Yu, P., Lin, T. C., Konigsberg, W. H., and Steitz, T. A. (1996) *Biochemistry 35*, 8110−8119.
6. Huang, W. H., and Lehman, I. R. (1992) *J. Biol. Chem. 247*, 3139−3146.
7. Kuchta, R. D., Benkovic, P., and Benkovic, S. J. (1988) *Biochemistry 27*, 6716−6725.
8. Han, H., Rifkind, J. M., and Mildvan, A. S. (1991) *Biochemistry 30*, 11104−11108.
9. Capson, T. L., Peliska, J. A., Kaboord, B. F., Frey, M. W., Lively, C., Dahlberg, M., and Benkovic, S. J. (1992) *Biochemistry 31*, 10984−10994.
10. Lin, T. C., Karam, G., and Konigsberg, W. H. (1994) *J. Biol. Chem. 269*, 19286−19294.
11. Bloom, L. B., Otto, M. R., Eritja, R., Reha-Krantz, L. J., Goodman, M. F., and Beechem, J. M. (1994) *Biochemistry 33*, 7576−7586.
12. Otto, M. R., Bloom, L. B., Goodman, M. F., and Beechem, J. M. (1998) *Biochemistry 37*, 10156−10163.
13. Joyce, C. M., and Steitz, T. A. (1987) *Trends Biochem. Sci. 12*, 288−292.
14. Eom, S. H., Wang, J., and Steitz, T. A. (1996) *Nature 382*, 278−281.
15. Reha-Krantz, L. J., and Nonay, R. L. (1993) *J. Biol. Chem. 268*, 27100−27108.
16. Reha-Krantz, L. J., Nonay, R. L., and Stocki, S. (1993) *J. Virol. 67*, 60−66.
17. Reha-Krantz, L. J., Stocki, S., Nonay, R. L., Eliosa, Dimayuga, E., Goodrich, L. D., Konigsberg, W. H., and Spicer, E. K. (1991) *Proc. Natl. Acad. Sci. U.S.A. 88*, 2417−2421.
18. Connolly, B. A. (1991) in *Oligonucleotides and analogues: A practical approach* (Eckstein, F., Ed.) pp 162−168, IRL Press, Oxford, England.
19. Kunkel, T. A., Eckstein, F., Mildvan, A. S., Koplitz, R. M., and Loeb, L. A. (1981) *Proc. Natl. Acad. Sci. U.S.A. 78*, 6734−6738.
20. Gupta, A. P., and Benkovic, S. J. (1984) *Biochemistry 23*, 5874−5881.
21. Weber, G. (1992) *Protein Interactions*, pp 15−16, Chapman and Hall, New York.
22. Bloom, L. B., Otto, M. R., Beechem, J. M., and Goodman, M. F. (1993) *Biochemistry 32*, 11247−11258.
23. Beechem, J. M., Gratton, E., Ameloot, M., Knutson, J. R., and Brand, L. (1991) The global analysis of fluorescence decay intensity and anisotropy decay data: Second generation theory and programs, in *Fluorescence spectroscopy: Principles* (Lakowicz, J. R., Ed.) Vol. II, Chapter V, Plenum Press, New York.
24. Landaw, E. M., and DiStefano, J. J., III (1984) *Am. J. Physiol. 246*, R665−R677.
25. Lakowicz, J. R. (1983) *Principles of Fluorescence Spectroscopy*, pp 257−301, Plenum Press, New York.
26. Reha-Krantz, L. J., and Nonay, R. L. (1994) *J. Biol. Chem. 269*, 5635−5643.
27. Stocki, S. A., Nonay, R. L., and Reha-Krantz, L. J. (1995) *J. Mol. Biol. 254*, 15−28.
28. Krugh, T. R. (1971) *Biochemistry 10*, 2594−2599.
29. Frey, M. W., Frey, S. T., Horrocks, W. D., Jr., Kaboord, B. F., and Benkovic, S. J. (1996) *Chem. Biol. 3*, 393−403.
30. Mullen, G. P., Serpersu, E. H., Ferrin, L. J., Loeb, L. A., and Mildvan, A. S. (1990) *J. Biol. Chem. 265*, 14327−14334.
31. Fothergill, M., Goodman, M. F., Petruska, J., and Warshel, A. (1995) *J. Am. Chem.* Soc. *117*, 11619−11627.
32. Clayton, L. K., Goodman, M. F., Branscomb, E. W., and Galas, D. J. (1979) *J. Biol. Chem. 254*, 1902−1912.

BI980074B